Measurement 224 (2024) 113883

Contents lists available at ScienceDirect

Measurement

journal homepage: www.elsevier.com/locate/measurement

Additional damping force identification of passively controlled structures based on a Gillijn De Moor filter

Xianzhi Li [a], Rui Zhang [a,b], Chunfeng Wan [c], Songtao Xue [a,d], Liyu Xie [a,*], Yunjia Tong [a]

[a] Department of Disaster Mitigation for Structures, Tongji University, Shanghai, China
[b] Department of Civil and Environmental Engineering, The Pennsylvania State University, University Park, PA, USA
[c] Southeast University, Key Laboratory of Concrete and Pre-Stressed Concrete Structure of Ministry of Education, Nanjing, China
[d] Department of Architecture, Tohoku Institute of Technology, Sendai, Japan

ARTICLE INFO

Keywords:
Additional damping force
Identification
Gillijn De Moor filter
Damper

ABSTRACT

The damping force provided by the damper is difficult to measure directly due to the complex mechanism of the damper in the structure. For damper-controlled structures, the additional damping force generated by the dampers can be considered a kind of input force on the primary structure. On the condition that the excitation force and parameters of the primary structure are known, an inverse method based on a Gillijn De Moor filter and structural response is presented in this paper to estimate the additional damping force. The state-space equations of damper-controlled structures are built first. The Gillijn De Moor filter is then used to estimate the additional damping force. The proposed method is examined by numerical simulations and a series of experiments. The results show that the additional damping force generated by dampers can be accurately estimated using the inverse method based on the Gillijn De Moor filter.

1. Introduction

In the past several decades, various energy dissipation devices have been developed and utilized to attenuate vibrations. The energy dissipation structures are usually equipped with dampers to absorb and dissipate energy, thereby enhancing the structural capacity for bearing and achieving the goal of structural control [1–4]. Energy dissipation devices such as dampers can be viewed as the "fuse" of structures, and their ability to dissipate energy plays a critical role in improving structural performance. Employing the appropriate types and quantities of dampers within a structure can significantly reduce the vibration response, thereby improving the seismic resistance of the structure and protecting the structure as well as its internal equipment from vibration-induced damage. However, the dampers may sometimes experience performance degradation or damage during long-term service, especially during the earthquakes. For example, after the Tohoku-oki earthquake (the largest earthquake in Japan's recorded history) on March 11, 2011, some dampers installed in buildings were damaged and cannot continue to protect the structure. Some dampers have experienced displacement far beyond their working stroke, causing damage to the damper support and piston detachment. Additionally, some high-strength bolts, crucial for damper fixation, had become loose, resulting in the damper no longer providing damping force. In addition, some sealing materials of oil dampers also experience severe wear and oil leakage during earthquakes, resulting in the loss of energy dissipation and vibration reduction ability of oil dampers [5–7]. When the dampers are degraded or damaged, they no longer provide sufficient protection for the structure, which will have a negative impact on structural safety. This condition underscores the crucial need for in-depth studies on damper performance within structures.

Identifying damper characteristics in structures has always been a challenging problem and received much attention [8,9]. Various methods have been developed for damper-controlled structures to identify structural damping ratios, which can be divided into frequency-domain and time-domain methods [10]. Furthermore, the additional damping force provided by dampers can directly describe the actual performance and energy dissipation capacity of control devices [11]. However, measuring the damping force directly in practice is not easy. As the structural responses are much more accessible, the additional damping force provided by the dampers can be considered a kind of input force on the primary structure, and the problem of additional damping force identification can be converted to a problem of input force identification [12,13]. The nonlinear hysteresis force provided by the base isolation system can also be treated as an additional unknown

* Corresponding author at: Department of Disaster Mitigation for Structures, Tongji University, Shanghai 200092, China.
E-mail address: liyuxie@tongji.edu.cn (L. Xie).

https://doi.org/10.1016/j.measurement.2023.113883
Received 6 April 2023; Received in revised form 22 October 2023; Accepted 15 November 2023
Available online 17 November 2023

input to the corresponding structural systems without base isolation [14]. Then, indirect estimation methods can be utilized to solve inverse problems involving force identification from the measurements of system responses [15]. The reference [12] also conducted a two-stage method to identify the force provided by the MR damper since the additional damping force generated by the dampers and unknown story stiffness parameters where the dampers are installed cannot be identified simultaneously. The identification of linear building structure parameters and seismic excitation is conducted in the first stage, and then the identification of MR damper forces is implemented in the second stage.

Some scholars have summarized the structural system identification problems and force estimation methods [16,17]. For example, Chan et al. developed a solution to solve the problem of tracking maneuvering targets using the generalized least-squares approach [18]. However, this input estimation algorithm has a batch form, which requires matrix inversions that result in computational inefficiency. Some inverse algorithms based on the Kalman filter (KF) have been developed to solve the problem of force identification. The KF was first proposed in 1960 and models the dynamic system into state equations [19]. The classical Kalman filter requires all the structural parameters and external input information to be available [20]. In terms of external input estimation, Hwang et al. developed a Kalman-based method to identify external input using the generalized inverse of matrix [21,22]. Ji et al. developed an input estimation algorithm, which consists of a KF and a recursive least squares algorithm, and it has shown great performance in tracking targets and computational efficiency [23]. To preserve the updating ability of the algorithm based on a KF method, forgetting factors are often utilized to modify the weighting matrix in the recursive least square algorithm [24]. Some algorithms with forgetting factors have been applied in structural systems, and the results have shown that the force estimations are in good agreement with theoretical results or measurements [25,26]. These input estimation methods provide the possibility to identify the unknown damping force of dampers in structure.

Since traditional KF-based identification methods usually need input information, they are not applicable when the additional damping force provided by the damper in the structure is unknown. In this regard, some Kalman filter methods with unknown input have been proposed. Lourens et al. proposed an augmented Kalman filters (AKF) method for force identification [27]. The method combines the unknown input with the state vector, and simultaneously estimates the system state and unknown input to the structure. However, the AKF method can be unstable, and Neats et al. studied the stability of the Kalman-based force estimation techniques and proposed some improved methods [28]. Maes et al. studied the joint state and input estimation method based on a limited number of response measurements [29]. Hassanabadi et al. proposed a Bayesian smoothing method for input-state estimation of linear structural systems without direct feedthrough [30]. Lei et al. also conducted research on the simultaneous identification of structural systems and unknown input, and the methods can be used in the case of unknown seismic inputs where the observation equations contain the absolute floor accelerations [31,32]. He et al. introduced a projection matrix that eliminated the unknown input in the observation equation, which ensured that the recognition of the state remained unaffected by the unknown input. Subsequently, they identified the unknown input using the posterior state [33,34]. Liu et al. also proposed some improved Kalman methods with unknown input. The data fusion of structural acceleration and displacement responses is used in the observations to avoid the low-frequency drift problem [35,36]. These methods allow for the recursive identification of the structural state and unknown input. However, the algorithm process is still relatively complex, which limits the application of these methods.

In recent years, Gillijns and De Moor developed a recursive optimal filter of joint state and input estimation for linear systems with direct transmission, which was originally proposed for optimal control applications [37,38]. The method can be applied to direct feedthrough systems, which means it can utilize the structural acceleration response as the measurements during the identification process. Lourens et al. further developed algorithms based on Gillijns De Moor filter (GDF) to reduce the numerical instability that occurs when the number of sensors exceeds the order of the model [39], allowing GDF to be applied to joint identification of structural state and input in large-scale civil engineering. The GDF also has the structure of a KF, except that an optimal estimate replaces the true value of the input. The input and state identified by the GDF are optimal in a minimum-variance unbiased sense. In this paper, an additional damping force identification method based on the GDF is developed. Input and state estimation can be jointly achieved by including the unknown additional damping forces in the state vector and estimating this augmented vector using the GDF method. It should be noted that the GDF-based method is applicable on the condition that the excitation force and parameters of the primary structure are known and structural acceleration responses at locations where additional damping forces generated are observed. In such case, the Gillijn De Moor filter could be directly adopted to identify the additional damping force. The effectiveness of the proposed GDF-based identification method is verified by numerical simulations of a damper-controlled MDOF system and laboratory experiments of a damper-equipped SDOF steel frame.

2. Additional damping force identification method

2.1. State equation of the system

For structures incorporated with dampers, the additional damping force provided by the dampers can be considered an unknown input force on the structure. Therefore, the equation of motion for the structures incorporated with dampers can be represented as:

$$\boldsymbol{M}_p\ddot{\boldsymbol{Y}}(t)+\boldsymbol{C}_p\dot{\boldsymbol{Y}}(t)+\boldsymbol{K}_p\boldsymbol{Y}(t)=\boldsymbol{L}_d\boldsymbol{G}(t)-\boldsymbol{M}_p\boldsymbol{I}_{n\times 1}\ddot{x}_g \tag{1}$$

where $\boldsymbol{M}_p$, $\boldsymbol{C}_p$ and $\boldsymbol{K}_p$ denote the mass matrix, damping matrix and stiffness matrix of the primary structure, respectively. $\boldsymbol{L}_d$ is the position matrix of dampers and $\boldsymbol{G}(t)$ is the additional damping force vector. $\boldsymbol{I}_{n\times 1}$ is a n-dimensional column vector and $\ddot{x}_g$ is the ground acceleration.$\boldsymbol{Y}(t)$, $\dot{\boldsymbol{Y}}(t)$ and $\ddot{\boldsymbol{Y}}(t)$ represent the displacement, velocity, and acceleration vectors, respectively.

In converting to the state-space model, the state vector of the dynamic system can be represented as $\boldsymbol{X}(t)=\left[\boldsymbol{Y}(t)\dot{\boldsymbol{Y}}(t)\right]^{\boldsymbol{T}}$, and the continuous-time state space model can be described as:

$$\dot{\boldsymbol{X}}(t)=\boldsymbol{A}\boldsymbol{X}(t)+\boldsymbol{B}\boldsymbol{F}(t)+\boldsymbol{B}\boldsymbol{L}_d\boldsymbol{G}(t) \tag{2}$$

where

$$\boldsymbol{A}=\begin{bmatrix}\boldsymbol{0} & \boldsymbol{I}\\ -\boldsymbol{M}_p^{-1}\boldsymbol{K}_p & -\boldsymbol{M}_p^{-1}\boldsymbol{C}_p\end{bmatrix},\ \boldsymbol{B}=\begin{bmatrix}\boldsymbol{0}\\ \boldsymbol{M}_p^{-1}\end{bmatrix},\ \boldsymbol{F}(t)=-\boldsymbol{M}_p\boldsymbol{I}_{n\times 1}\ddot{x}_g \tag{3}$$

Eq. (2) can be discretized over time intervals of length Δt, and combined with noise inputs, Eq. (2) can be written as:

$$\boldsymbol{X}_{k+1}=\boldsymbol{\Phi}\boldsymbol{X}_k+\boldsymbol{\Gamma}\boldsymbol{F}_k+\boldsymbol{\Gamma}\boldsymbol{L}_d\boldsymbol{G}_k+\boldsymbol{\omega}_k \tag{4}$$

where

$$\begin{aligned}\boldsymbol{\Phi}&=\exp(\boldsymbol{A}\Delta t)\boldsymbol{\Gamma}=\int_{k\Delta t}^{(k+1)\Delta t}\exp\{\boldsymbol{A}[(k+1)\Delta t-\tau]\}d\tau\boldsymbol{B}\\&=[\boldsymbol{I}-\exp(-\boldsymbol{A}\Delta t)]\boldsymbol{A}^{-1}\boldsymbol{B}\end{aligned} \tag{5}$$

$\boldsymbol{\Phi}$ is the state transition matrix, $\boldsymbol{\Gamma}$ is the input matrix, $\boldsymbol{F}_k$ is the sequence of excitation force, $\boldsymbol{L}_d\boldsymbol{G}_k$ is the sequence of additional damping force, $\boldsymbol{\omega}_k$ is the process noise vector, which is assumed to be zero mean and white noise, and $\mathbf{Q}$ is the corresponding covariance matrix.

The recursive filter (GDF) developed by Gillijns and De Moor [37]

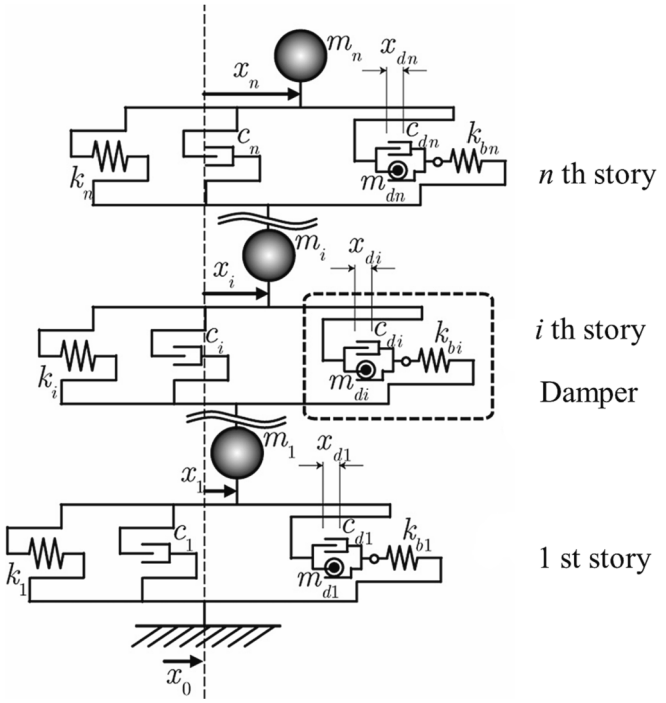

Fig. 1. Analytical model for the MDOF system incorporated with dampers.

Table 1
Parameters of the primary structure.

Story	Primary structure			Damper		
	Mass m_i(ton)	Stiffness k_i(kN/m)	Height (m)	Mass m_{di} (ton)	Stiffness k_{bi} (kN/m)	Damping c_{di} (kNs/m)
10	875	158,550	4	1626	20,138	2353
9	649	180,110	4	1847	22,877	2673
8	656	220,250	4	2259	27,975	3269
7	660	244,790	4	2511	31,092	3633
6	667	291,890	4	2994	37,075	4332
5	670	306,160	4	3140	38,887	4544
4	676	328,260	4	3367	41,694	4872
3	680	383,020	4	3929	48,650	5684
2	682	383,550	4	3934	48,717	5692
1	700	279,960	6	2872	35,560	4155

can be applied to a direct feedthrough system, using the structural acceleration and displacement responses as the observation measurements. Thus, as mentioned above, the measurement equation can be written as:

$$\boldsymbol{Z}_k = \boldsymbol{C}\boldsymbol{X}_k + \boldsymbol{H}\boldsymbol{F}_k + \boldsymbol{H}\boldsymbol{L}_d\boldsymbol{G}_k + \boldsymbol{\nu}_k \tag{6}$$

where

$$\boldsymbol{C} = \begin{bmatrix} \boldsymbol{I} & \boldsymbol{0} \\ -\boldsymbol{M}^{-1}\boldsymbol{K} & -\boldsymbol{M}^{-1}\boldsymbol{C} \end{bmatrix} \boldsymbol{H} = \begin{bmatrix} \boldsymbol{0} \\ \boldsymbol{M}^{-1} \end{bmatrix} \tag{7}$$

H is the measurement matrix, and $\boldsymbol{Z}_k$ is the observation vector that consists of structural displacement and acceleration responses. $\boldsymbol{\nu}_k$ is the measurement noise vector, which is assumed to be zero mean and white noise, and the corresponding covariance matrix is **R**. In this study, both structural acceleration and displacement can be selected as the observations. If only the structural acceleration responses are used as the observations, the identification results may sometimes appear low-frequency drift, but the identification results can be significantly improved when the observations include partial structural displacement. Therefore, it is suggested that both the structural acceleration and displacement responses be included in the observation vector to get better identification results.

2.2. Gillijn De Moor Filter (GDF)

The Gillijns De Moor Filter (GDF) has a Kalman filter structure, which can be described as a recursive three-step filter. The first step can be defined as a time update, using the given measurements at time $k-1$ and defining $\widehat{\boldsymbol{X}}_{k\text{-}1/k-1}$ and $\widehat{\boldsymbol{G}}_{k-1}$ as the optimal unbiased estimates of $\boldsymbol{X}_{k-1}$ and $\boldsymbol{G}_{k-1}$, respectively. The prediction at time k can be obtained:

$$\widehat{\boldsymbol{X}}_{k/k-1} = \boldsymbol{\Phi}\widehat{\boldsymbol{X}}_{k-1/k-1} + \boldsymbol{\Gamma}\boldsymbol{F}_{k-1} + \boldsymbol{\Gamma}\boldsymbol{L}_d\widehat{\boldsymbol{G}}_{k-1} \tag{8}$$

$$\boldsymbol{P}^{x}_{k/k-1} = [\boldsymbol{\Phi} \quad \boldsymbol{\Gamma}] \begin{bmatrix} \boldsymbol{P}^{x}_{k-1/k-1} & \boldsymbol{P}^{xG}_{k-1} \\ \boldsymbol{P}^{Gx}_{k-1} & \boldsymbol{P}^{G}_{k-1} \end{bmatrix} \begin{bmatrix} \boldsymbol{\Phi}^T \\ \boldsymbol{\Gamma}^T \end{bmatrix} + \boldsymbol{Q}_{k-1} \tag{9}$$

where $\boldsymbol{P}^{x}_{k/k-1}$ represents the covariance matrix of $\widehat{\boldsymbol{X}}_{k/k-1}$, $\boldsymbol{P}^{x}_{k/k-1} = \boldsymbol{E}\left[(\boldsymbol{X}_k - \widehat{\boldsymbol{X}}_{k/k-1})(\boldsymbol{X}_k - \widehat{\boldsymbol{X}}_{k/k-1})^T\right]$.

The second step can be defined as input estimation. The unbiased estimate of $\boldsymbol{L}_d\boldsymbol{G}_k$ can be calculated by weighted least square estimation, and the weighting matrix equals the inverse of $\widetilde{\boldsymbol{R}}_k$.

$$\boldsymbol{L}_d\widehat{\boldsymbol{G}}_k = \boldsymbol{M}_k(\boldsymbol{Z}_k - \boldsymbol{C}\widehat{\boldsymbol{X}}_{k/k-1} - \boldsymbol{H}\boldsymbol{F}_k) \tag{10}$$

$$\boldsymbol{M}_k = (\boldsymbol{H}^T\widetilde{\boldsymbol{R}}_k^{-1}\boldsymbol{H})^{-1}\boldsymbol{H}^T\widetilde{\boldsymbol{R}}_k^{-1} \tag{11}$$

$$\widetilde{\boldsymbol{R}}_k = \boldsymbol{C}\boldsymbol{P}^{x}_{k/k-1}\boldsymbol{C}^T + \boldsymbol{R}_k \tag{12}$$

$$\boldsymbol{P}^{G}_{k} = (\boldsymbol{H}^T\widetilde{\boldsymbol{R}}_k^{-1}\boldsymbol{H})^{-1} \tag{13}$$

where $\boldsymbol{P}^{G}_{k}$ represents the covariance matrix of $\boldsymbol{L}_d\widehat{\boldsymbol{G}}_k$, $\boldsymbol{P}^{G}_{k} = \boldsymbol{E}\left[(\boldsymbol{L}_d\boldsymbol{G}_k - \boldsymbol{L}_d\widehat{\boldsymbol{G}}_k)(\boldsymbol{L}_d\boldsymbol{G}_k - \boldsymbol{L}_d\widehat{\boldsymbol{G}}_k)^T\right]$.

The third step can be defined as a measurement update. The update of $\widehat{\boldsymbol{X}}_{k/k-1}$ with the measurement $\boldsymbol{Z}_k$ at time k can be obtained:

$$\widehat{\boldsymbol{X}}_{k/k} = \widehat{\boldsymbol{X}}_{k/k-1} + \boldsymbol{K}_k(\boldsymbol{Z}_k - \boldsymbol{C}\widehat{\boldsymbol{X}}_{k/k-1} - \boldsymbol{H}\boldsymbol{F}_k - \boldsymbol{H}\boldsymbol{L}_d\widehat{\boldsymbol{G}}_k) \tag{14}$$

$$\boldsymbol{K}_k = \boldsymbol{P}^{x}_{k/k-1}\boldsymbol{C}^T\widetilde{\boldsymbol{R}}_k^{-1} \tag{15}$$

$$\boldsymbol{P}^{x}_{k/k} = \boldsymbol{P}^{x}_{k/k-1} - \boldsymbol{K}_k(\widetilde{\boldsymbol{R}}_k - \boldsymbol{H}\boldsymbol{P}^{G}_{k}\boldsymbol{H}^T)\boldsymbol{K}_k^T \tag{16}$$

$$\boldsymbol{P}^{xG}_{k} = (\boldsymbol{P}^{Gx}_{k})^T = \boldsymbol{K}_k\boldsymbol{H}\boldsymbol{P}^{G}_{k} \tag{17}$$

where $\boldsymbol{K}_k$ is the gain, $\boldsymbol{P}^{x}_{k/k} = \boldsymbol{E}\left[(\boldsymbol{X}_k - \widehat{\boldsymbol{X}}_{k/k})(\boldsymbol{X}_k - \widehat{\boldsymbol{X}}_{k/k})^T\right]$, and $\boldsymbol{P}^{Gx}_{k} = \boldsymbol{E}\left[(\boldsymbol{L}_d\boldsymbol{G}_k - \boldsymbol{L}_d\widehat{\boldsymbol{G}}_k)(\boldsymbol{X}_k - \widehat{\boldsymbol{X}}_{k/k})^T\right]$.

2.3. Summary of GDF equations

In conclusion, the procedure to estimate the additional damping force can be summarized as follows:

(1) The state space Eqs. (3) and (6) are established, and the state vector is clarified, which represents the structural responses;
(2) Based on Eqs. (8) and (9), the estimate of $\boldsymbol{X}_k$ given measurements up to time $k-1$ can be obtained, that is, $\widehat{\boldsymbol{X}}_{k/k-1}$;
(3) With $\widehat{\boldsymbol{X}}_{k/k-1}$ and its covariance matrix $\boldsymbol{P}^{x}_{k/k-1}$, the unbiased estimate of $\boldsymbol{L}_d\boldsymbol{G}_k$ can be obtained based on Eqs. (10) to (13), that is, $\boldsymbol{L}_d\widehat{\boldsymbol{G}}_k$;
(4) Finally, the estimate of $\boldsymbol{X}_k$ given measurements up to time k can be obtained based on Eqs. (14) to (17), that is, $\widehat{\boldsymbol{X}}_{k/k}$.

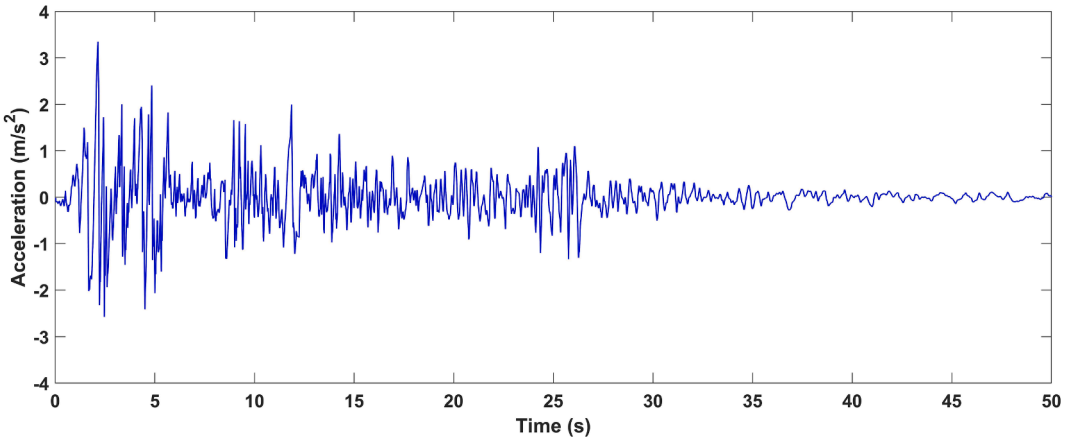

Fig. 2. The time-history curve of acceleration of EI Centro Earthquake.

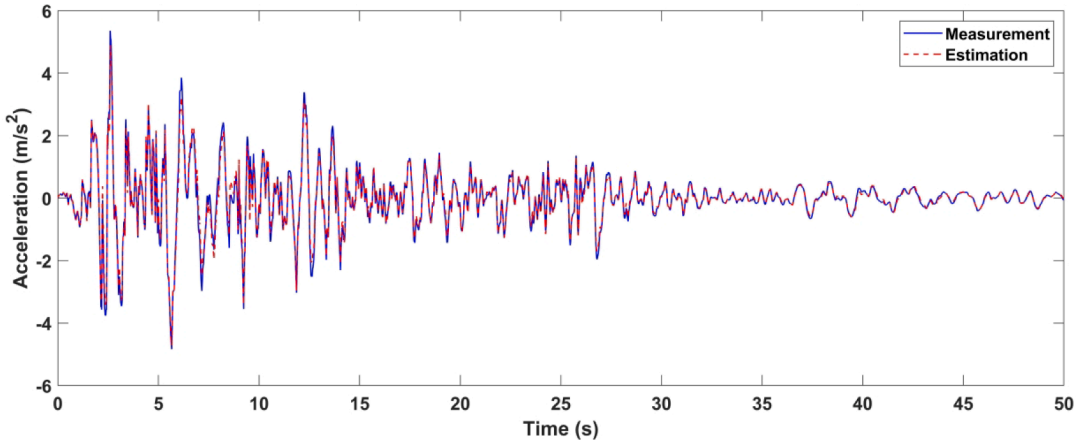

Fig. 3. Acceleration response of structure incorporated with dampers (10th floor).

3. Numerical simulations and results

To validate the efficiency of the GDF-based identification method for state estimation and additional damping force estimation, numerical simulations of an MDOF structural system are carried out.

3.1. The MDOF system incorporated with dampers

In this study, a 10-story benchmark structure developed by the Japan Society of Seismic Isolation is adopted as a vibration control analysis example [40]. The analytical model of the 10-story benchmark structure is detailed in Fig. 1 and Table 1. Every story of the structure is equipped with a damper. Thus, there are additional damping forces at each floor level, and each floor level additional damping forces are different. m_i, c_i, and k_i denote the mass, damping, and stiffness of the ith story, respectively. m_{di}, c_{di}, and k_{di} denote the mass, damping, and stiffness of the damper installed in the ith story, respectively. The equation of motion for the structure can be represented as Eq. (1). Correspondingly, $\boldsymbol{Y}(t)$ is the displacement vector of the structure relative to the ground.

$$\boldsymbol{M}_p = \begin{bmatrix} m_1 & 0 & \cdots & 0 \\ 0 & m_1 & & \vdots \\ \vdots & & \ddots & 0 \\ 0 & \cdots & 0 & m_n \end{bmatrix} \tag{18}$$

$$\boldsymbol{K}_p = \begin{bmatrix} k_1+k_2 & -k_2 & 0 & \cdots & 0 \\ -k_2 & k_2+k_3 & -k_3 & & \vdots \\ 0 & & \ddots & & 0 \\ \vdots & & -k_{n-1} & k_{n-1}+k_n & -k_n \\ 0 & \cdots & 0 & -k_n & k_n \end{bmatrix} \tag{19}$$

$$\boldsymbol{C}_p = \frac{2\xi_1}{\omega_{p1}}\boldsymbol{K}_p \tag{20}$$

$$\boldsymbol{G}(t) = k_b x_b = m_d \ddot{x}_d + c_d \dot{x}_d \tag{21}$$

where ξ_1 and ω_{p1} denote the damping ratio for the 1st mode and the lowest fundamental angular frequency of the primary structure, respectively. In this study, ξ_1 equals 0.02 and ω_{p1} equals 3.13 Hz. k_b and x_b denote the stiffness and displacement of the spring, respectively. m_d, c_d and x_d denote the mass, damping and displacement of the damper, respectively. The displacement of the structure relative to the ground equals x_b plus x_d.

3.2. Additional damping force identification

The EI Centro earthquake is used as the ground excitation in the numerical stimulation (Fig. 2). The acceleration and displacement responses are calculated using the Newmark-beta algorithm and considered observations for the identification problem.

The GDF-based identification method is then adopted to estimate the state and the additional damping force generated by dampers. In the numerical example, the additional damping forces at each story are

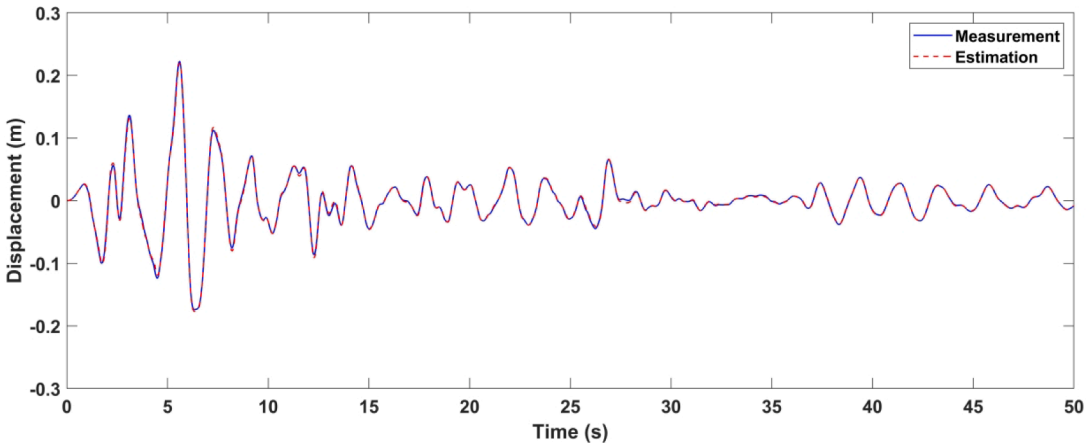

Fig. 4. Displacement response of structure incorporated with dampers (10th floor).

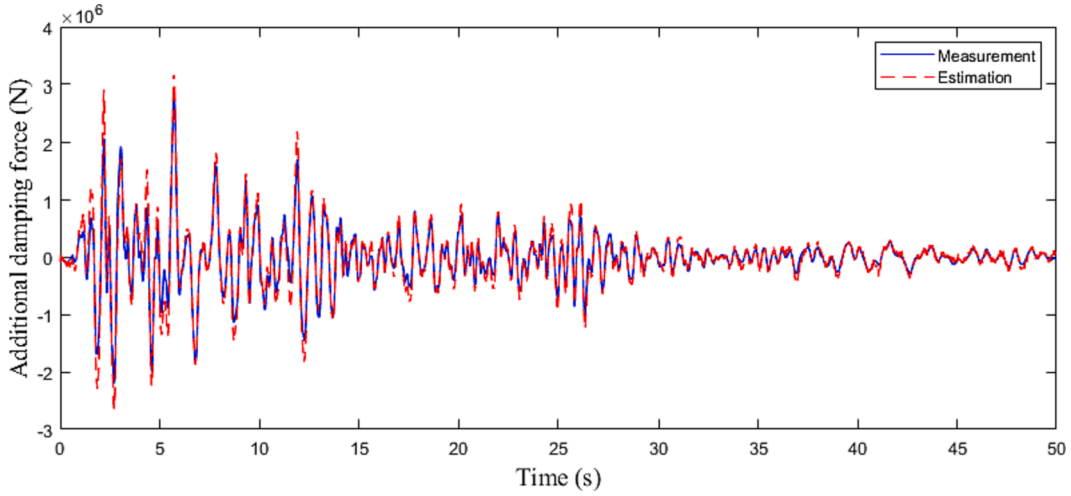

Fig. 5. The theoretical and estimated additional damping forces (2nd floor).

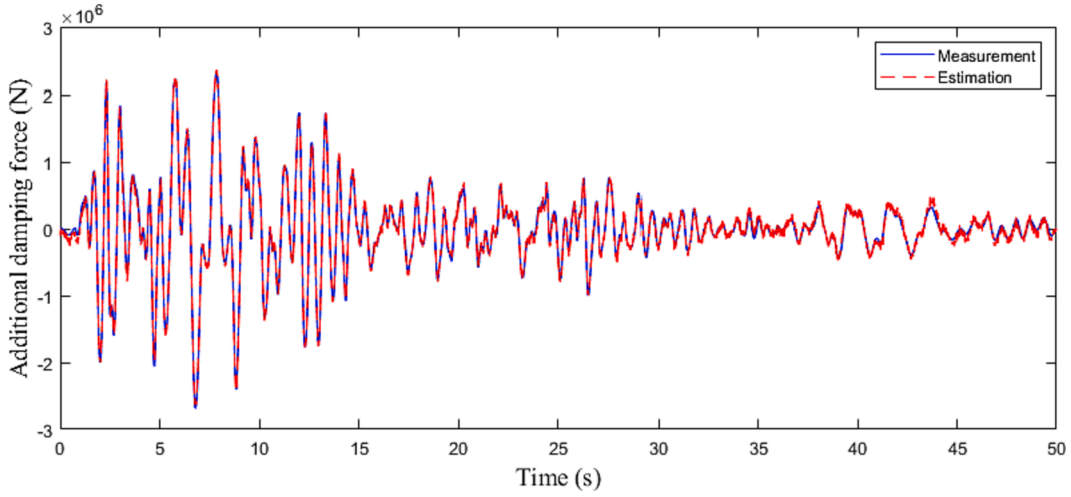

Fig. 6. The theoretical and estimated additional damping forces (5th floor).

different, and the acceleration responses need to be observed at each story where the dampers are installed. Therefore, ten story acceleration responses of the structure are observed to identify the additional damping forces at each story. In addition, the structural displacement responses of the 1st, 3rd, 5th, 7th, and 10th floors are also included in the observation to avoid drift problems and make the identification results more accurate. In the numerical examples, the structural response measurements all contain Gaussian white noise with 2 % noise-to-signal ratio in root mean square (RMS). The initial values used in the GDF-based identification method are given as follows: sampling interval $\Delta t =$

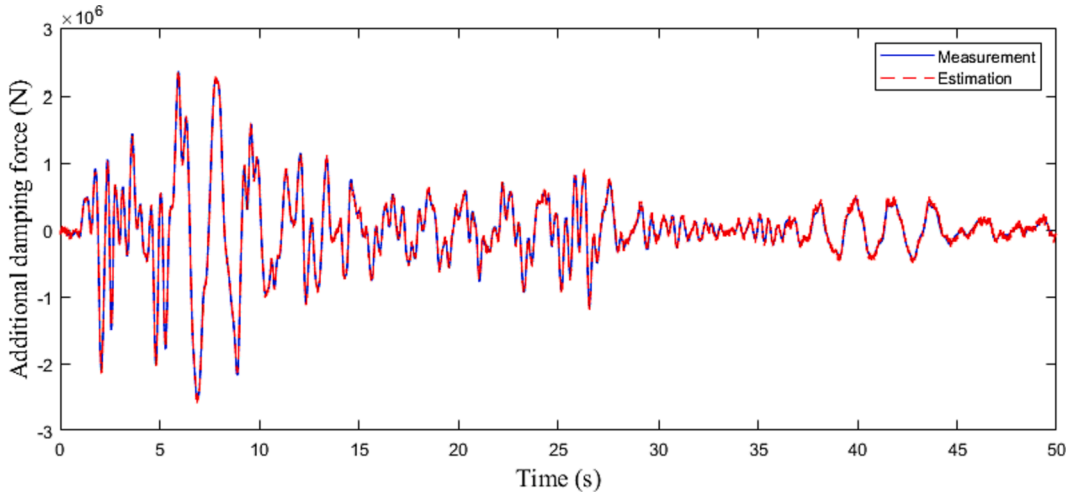

Fig. 7. The theoretical and estimated additional damping forces (7th floor).

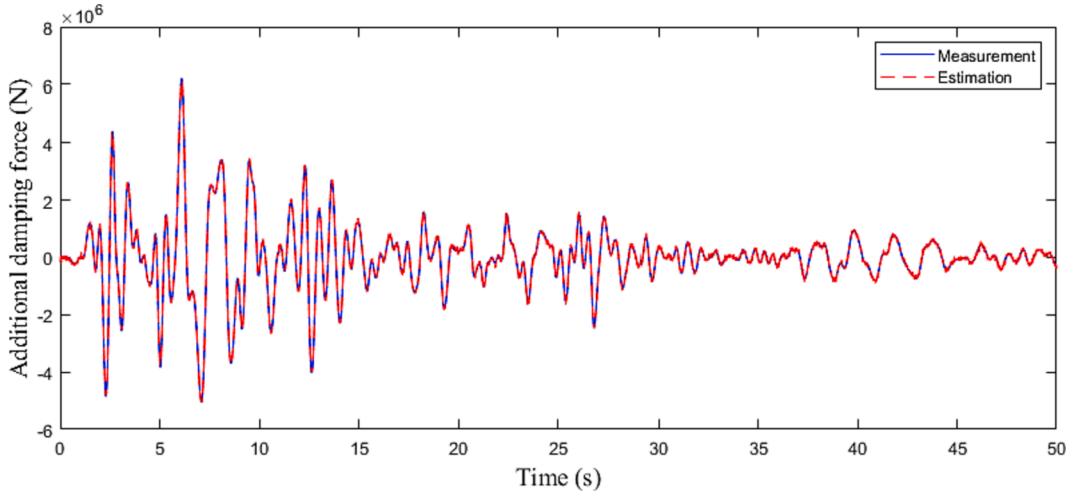

Fig. 8. The theoretical and estimated additional damping forces (10th floor).

Table 2
The relative root means square error of all identified additional damping forces.

Story	Error (%)	Story	Error (%)
1	15.84	**6**	8.68
2	17.56	**7**	7.76
3	10.86	**8**	6.44
4	9.71	**9**	6.79
5	9.44	**10**	7.36

10^{-3}s, covariance matrix of process noise $\mathbf{Q} = 10^{-18} \cdot \boldsymbol{I}_{20\times20}$, covariance matrix of measurement noise $\mathbf{R} = 10^{-12} \cdot \boldsymbol{I}_{20\times20}$, initial state vector $\widehat{\boldsymbol{X}}_0 = \mathbf{0}_{20\times1}$, initial additional damping force state vector $\widehat{\boldsymbol{G}}_0 = \mathbf{0}_{10\times1}$, initial covariance matrixes $\boldsymbol{P}_0^x = 1 \times 10^{20} \cdot \boldsymbol{I}_{20\times20}$. Through analysis, the estimated responses and additional damping force can be seen in Figs. 3 to 8, and the relative root mean square error of all identified additional damping forces are shown in Table 2. The theoretical additional damping force is calculated by Eq. (21). The results show that the GDF-based identification method has a good tracking capability by contrasting the estimation and the calculated measurements.

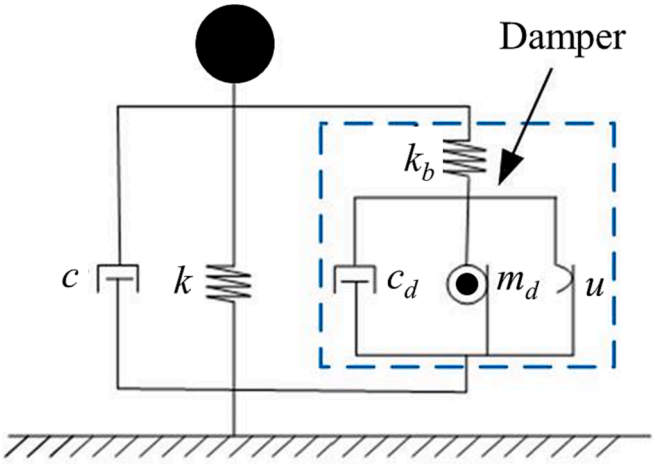

Fig. 9. Analytical model for the SDOF system incorporated with the damper.

4. Experimental verification and results

In this section, the structural responses and the additional damping force of a damper-controlled SDOF steel frame are estimated through a

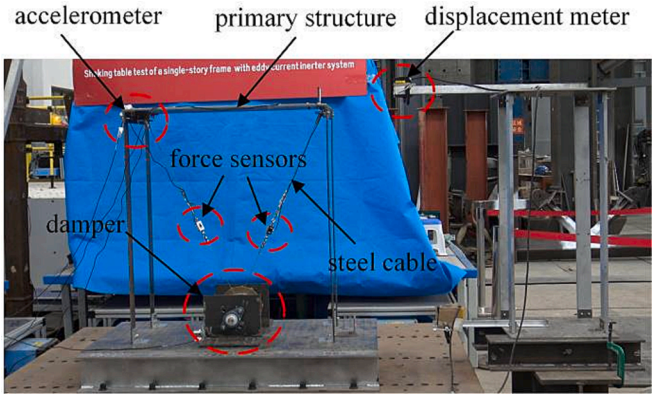

Fig. 10. Configuration of the test specimen.

series of experiments using the GDF-based identification method.

4.1. Experimental equipment

The experimental model consists of the primary structure and the damper (Fig. 9). The primary structure is an SDOF steel frame, and the mass and height of the primary structure are 23 kg and 1.0 m, respectively. The total height of the SDOF structure is 1.000 m. The top plate consists of steel plates (Q245) with plane dimensions of 0.834 × 0.390 m and a thickness of 0.01 m. The columns consist of steel plates (Q245) with height × width × thickness dimensions of 1.000 × 0.150 × 0.003 m. The first natural frequency of the primary structure is adjusted to almost 1 Hz. The damper is connected to the primary structure with steel cables. The experiment uses the free vibration method, with an initial displacement of 80 mm. An accelerometer and a displacement meter are installed to measure the acceleration and displacement of the top floor. Two force sensors are stalled in the steel cables to measure the tension of the steel cables (Fig. 10).

4.2. Parameter identification of primary structure using extended Kalman filter

Since the proposed GDF-based additional damping force identification method is only applicable when the structural parameters are known, the stiffness and damping of the primary structure must be identified first to calculate the additional damping force provided by the damper. The additional damping force generated by the dampers and unknown structural parameters where the dampers are installed cannot be identified simultaneously. In reference [12], the linear structure parameters are also identified in the first stage. Therefore, in this experimental study, the extended Kalman filter (EKF) is adopted first to identify the stiffness and damping of the primary structure under the condition that the external excitation is already known.

The free vibration test of the primary structure without the damper is conducted first. The equation of motion for the primary structure can be represented as:

$$m\ddot{\boldsymbol{Y}}(t)+c\dot{\boldsymbol{Y}}(t)+k\boldsymbol{Y}(t)=\boldsymbol{0} \tag{22}$$

where m, c and k denote the mass, damping and stiffness of the primary structure, respectively.

In the EFK algorithm, the extended state vector can be defined as:

$$\dot{\boldsymbol{X}}=\left\{\dot{\boldsymbol{X}}_1 \quad \dot{\boldsymbol{X}}_2 \quad \dot{\boldsymbol{X}}_3 \quad \dot{\boldsymbol{X}}_4\right\}^T=\left\{\boldsymbol{X}_2 \quad m^{-1}(-c\boldsymbol{X}_2-k\boldsymbol{X}_1) \quad 0 \quad 0\right\}^T \tag{23}$$

where $\boldsymbol{X}_1=\boldsymbol{Y},\boldsymbol{X}_2=\dot{\boldsymbol{Y}},\boldsymbol{X}_3=k,\boldsymbol{X}_4=c$. In converting to the state-space model, the state space equation can be described as:

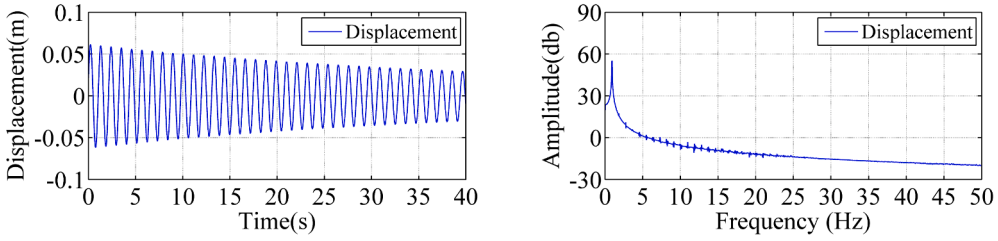

Fig. 11. Structural displacement response of the primary structure.

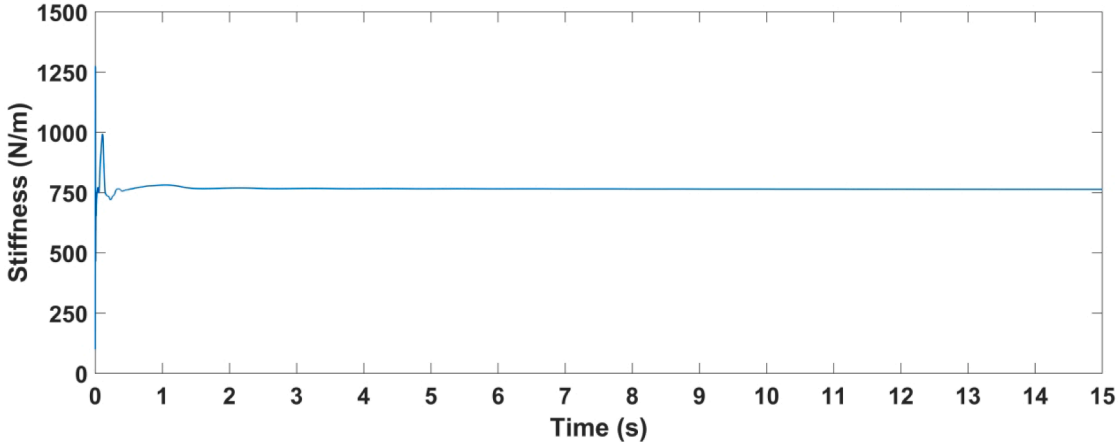

Fig. 12. Parameter estimation of primary structure: stiffness.

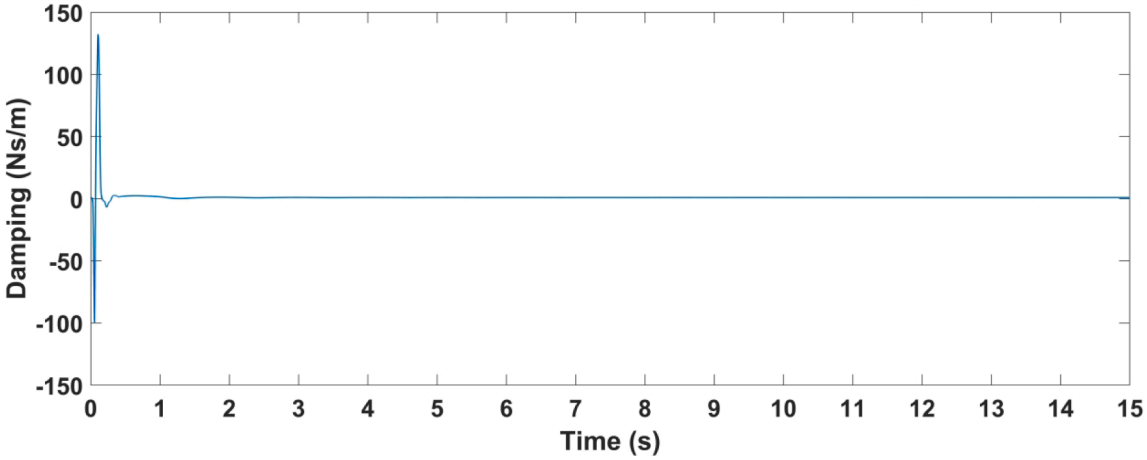

Fig. 13. Parameter estimation of primary structure: damping.

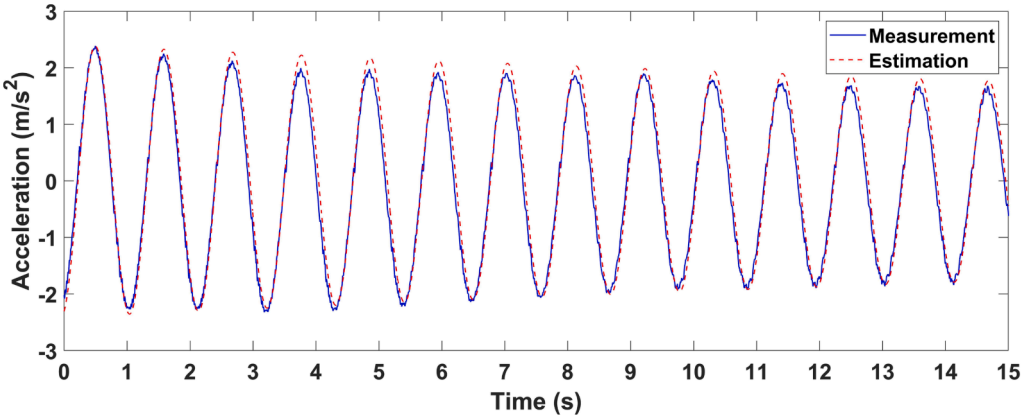

Fig. 14. Simulation comparison: structural acceleration response of the primary structure.

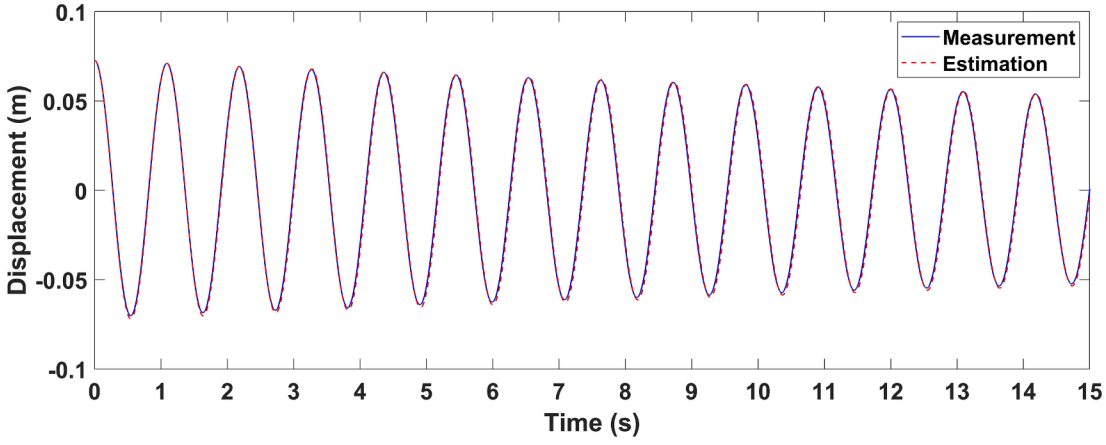

Fig. 15. Simulation comparison: structural displacement response of the primary structure.

$$\dot{\boldsymbol{X}} = f(\boldsymbol{X}, t) + \boldsymbol{\omega}(k) \tag{24}$$

$$\boldsymbol{Z}_k = h(\boldsymbol{X}_k, t_k) + \boldsymbol{v}_k \tag{25}$$

where $\boldsymbol{Z}_k$ is the observation vector at time k.

The key steps of EFK consist of the time update step and measurement update step. The nonlinear term $f(\boldsymbol{X}, t)$ in Eq. (24) can be linearized by Taylor's expansion. In the time update step, the predicted state at time k can be represented as:

$$\widehat{\boldsymbol{X}}_{k/k-1} = \widehat{\boldsymbol{X}}_{k-1/k-1} + \int_{t_{k-1}}^{t_k} f(\widehat{\boldsymbol{X}}_{k-1/k-1}, t)dt \tag{26}$$

In this study, the fourth-order Runge-Kutta algorithm method was utilized to resolve the differential equations. Since the Runge-Kutta algorithm is a widely-used numerical method, this article does not provide a detailed description of its solution process.

In the measurement update step, the updated state at time k can be

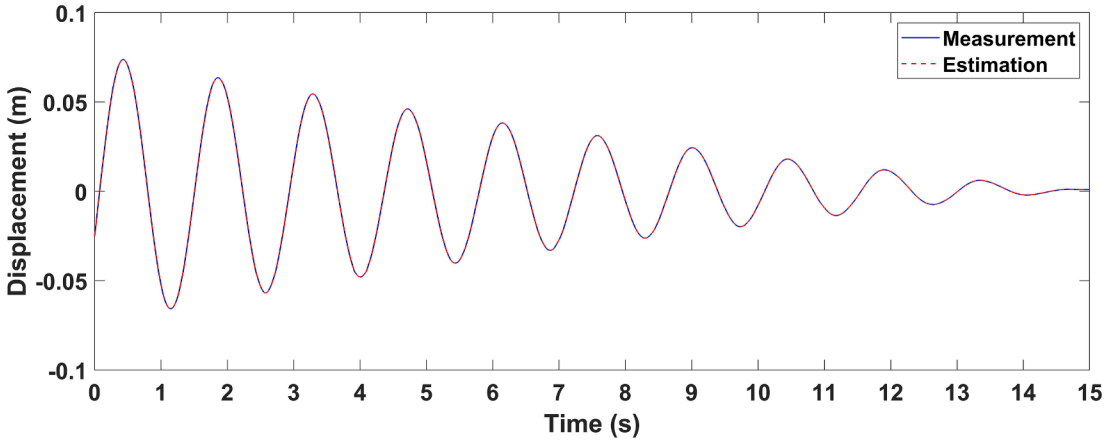

Fig. 16. Comparison of the identified and measured displacement responses of the structure incorporated with the damper.

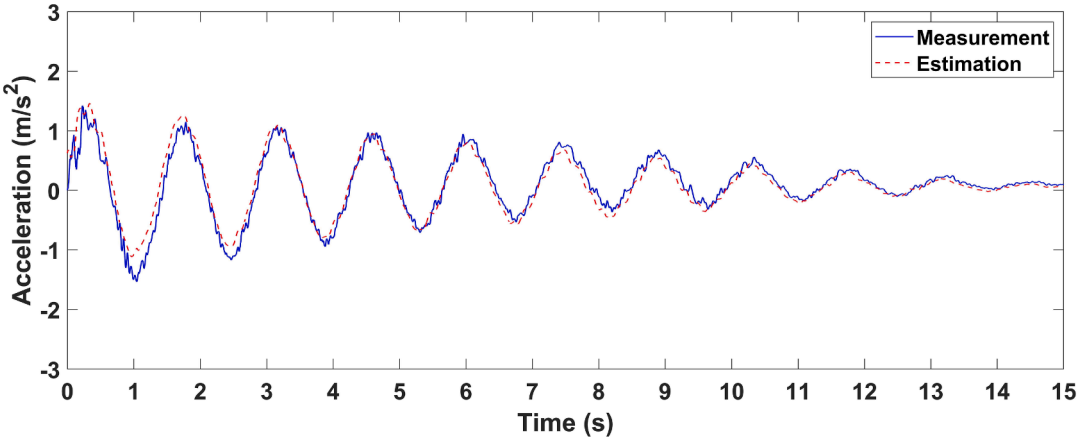

Fig. 17. Comparison of the identified and measured acceleration responses of the structure incorporated with the damper.

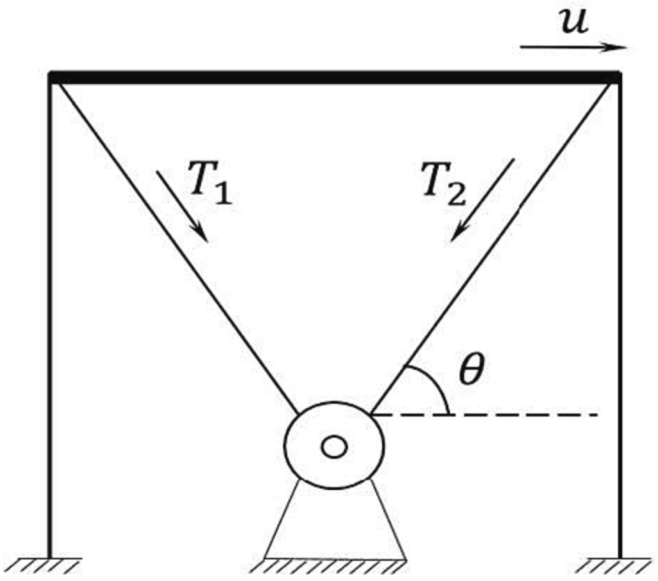

Fig. 18. Calculation principle of the additional damping force.

represented as:

$$\widehat{\boldsymbol{X}}_{k/k} = \widehat{\boldsymbol{X}}_{k/k-1} + \boldsymbol{K}_k\left[\boldsymbol{Z}_k - h(\widehat{\boldsymbol{X}}_{k/k-1}, t_k)\right] \tag{27}$$

where $\boldsymbol{K}_k$ is the Kalman gain.

In this study, the observation is the displacement response of the top floor, and the displacement response in both the time domain and frequency domain can be seen in Fig. 11. In Fig. 11a, the damping ratio can be calculated by using the logarithmic decrement method,

$$\xi = \frac{1}{2\pi n}\ln\frac{x_k}{x_{k+n}} \tag{28}$$

where x_k and x_{k+n} are displacement response amplitudes within n cycle intervals. The calculated damping ratio $\xi = 0.33\%$. In Fig. 11b, the natural frequency of the structure can be calculated as $f = 0.915$ Hz by using a fast Fourier transform.

The initial values used in the EFK are given as follows: sampling interval $\Delta t = 10^{-3}$s and covariance matrix of measurement noise $\mathbf{R} = 10^{-12}\cdot\boldsymbol{I}$. Initial state vector $\widehat{\boldsymbol{X}}_0 = \{0 \quad 0 \quad 1 \quad 10^2\}^T$, initial covariance matrixes $\boldsymbol{P}_0^x = \begin{bmatrix} 1 & 0 & 0 & 0 \\ 0 & 1 & 0 & 0 \\ 0 & 0 & 10 & 0 \\ 0 & 0 & 0 & 10^6 \end{bmatrix}$. The estimated stiffness and damping of the primary structure are shown in Figs. 12 and 13. The estimated k and c equal 762.232 N/m and 0.957 Ns/m, respectively. The corresponding estimations of the structural natural frequency and damping ratio are calculated as 0.916 Hz and 0.36 %, respectively, which are close to the theoretical values calculated previously using the fast

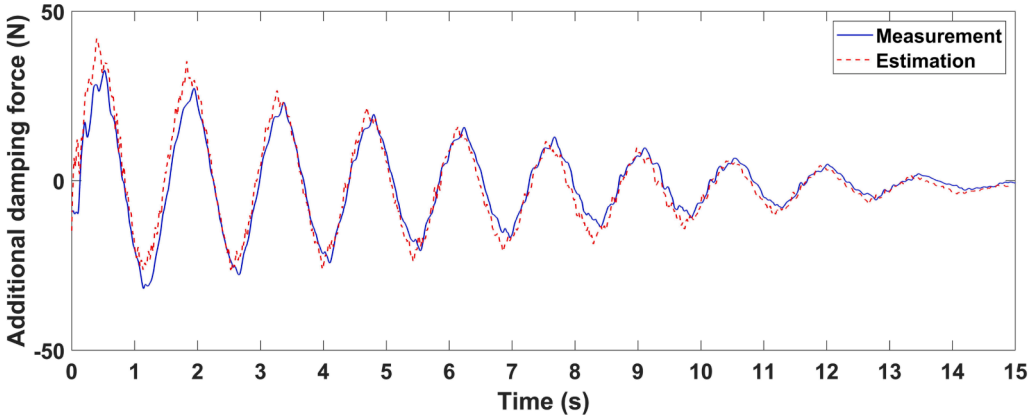

Fig. 19. Comparison between the measurement and estimation of additional damping force.

Fourier transform and logarithmic decrement method. An inversion analysis is also conducted to calculate the structural acceleration and displacement responses, and the estimated structural responses are close to the experimental measurements, which verifies the accuracy of the estimated parameters (Figs. 14 and 15).

4.3. Additional damping force identification

For the free vibration test of the structure with the damper, the equation of motion for the structure can be represented as:

$$m\ddot{\boldsymbol{Y}}(t)+c\dot{\boldsymbol{Y}}(t)+k\boldsymbol{Y}(t)=\boldsymbol{G}(t) \tag{29}$$

As mentioned above, the additional damping force identification algorithm based on GDF is utilized to estimate the additional damping force provided by the damper. The observations are the displacement and acceleration responses of the top floor. The initial values used in the GDF-based algorithm are given as follows: sampling interval $\Delta t = 10^{-3}$s, covariance matrix of process noise $\mathbf{Q}=10^{-2}\cdot\boldsymbol{I}$, covariance matrix of measurement noise $\mathbf{R}=10^{-10}\cdot\boldsymbol{I}$, initial state vector $\widehat{\boldsymbol{X}}_0=\boldsymbol{0}_{2\times1}$, initial additional damping force state vector $\widehat{\boldsymbol{G}}_0=\boldsymbol{0}_{1\times1}$, initial covariance matrixes $\boldsymbol{P}_0^x=1\times10^{20}\cdot\boldsymbol{I}_{2\times2}$. Figs. 16 and 17 show the comparisons of the estimated and measured time histories of the displacement and acceleration responses, respectively. It is shown that the structural responses can be identified with high accuracy using the GDF-based identification method.

The theoretical additional damping force $\widehat{G}$ can be calculated as:

$$\widehat{G}=(T_1-T_2)\cos\theta \tag{30}$$

where T_1 and T_2 are the tension in the steel cables measured by force sensors, and the calculation principle is shown in Fig. 18. The estimated results of the additional damping force based on the GDF and the theoretical results based on the measurement are compared in Fig. 19.

From the comparison between the measurement and estimation of the additional damping force, we can see that they are in good agreement. Although there are still some errors in the identified and the measured damping force in the initial stage, the relative root mean square error of the identified additional damping force is less than 20 %, which indicates that the identification results of additional damping forces have good accuracy. The reason for the errors may be the noise interference in the observation measurement. In addition, some errors may be caused by the differences between the actual structural parameters and the parameters identified using the EKF method in the previous stage.

5. Conclusions

In this paper, an inverse methodology based on the Gillijn De Moor filter is developed to estimate the state and the additional damping force generated by dampers. Numerical simulations examine the feasibility of the method. The numerical simulations adopt a ten-story structure incorporated with dampers. The results show that the proposed approach can estimate the state and unknown additional damping force. In addition, the proposed approach is validated by free vibration tests of an SDOF structure incorporated with a damper. The estimations of the additional damping force agree well with the theoretical results. The numerical and experimental results show that the additional damping force provided by dampers can be estimated with high accuracy using the inverse method based on Gillijn De Moor filter. Despite the encouraging results, some limitations still need to be addressed, such as the structural parameters need to be known or identified first. Furthermore, the acceleration responses at locations where the dampers are installed must be observed to accurately identify the additional damping forces provided by dampers.

Funding

The authors gratefully acknowledge the National Natural Science Foundation of China (51778490), the Natural Science Foundation of Shanghai (Grant No. 20ZR1461800) and The Key Program of Intergovernmental International Scientific and Technological Innovation Cooperation (2021YFE010033) for having guided and funded the research presented in this article.

CRediT authorship contribution statement

Xianzhi Li: Methodology, Writing – original draft, Writing – review & editing. **Rui Zhang:** Methodology, Software, Writing – original draft, Writing – review & editing. **Chunfeng Wan:** Validation, Writing – review & editing. **Songtao Xue:** Writing – review & editing, Project administration. **Liyu Xie:** Conceptualization, Methodology, Writing – original draft. **Yunjia Tong:** Writing – original draft.

Declaration of Competing Interest

The authors declare that they have no known competing financial interests or personal relationships that could have appeared to influence the work reported in this paper.

Data availability

Data will be made available on request.

References

[1] M. Symans, F. Charney, A. Whittaker, et al., Energy Dissipation Systems for Seismic Applications: Current Practice and Recent Developments, J. Struct. Eng. 134 (1) (2008) 3–21.
[2] G. Housner, L. Bergman, T. Caughey, et al., Structural Control: Past, Present, and Future, J. Eng. Mech. 123 (9) (1997) 897–971.
[3] S. Xue, J. Kang, L. Xie, et al., Cross-Layer Installed Cable-Bracing Inerter System for MDOF Structure Seismic Response Control, Appl. Sci. 10 (17) (2020) 5914.
[4] J. Kang, S. Xue, L. Xie, et al., Multi-modal seismic control design for multi-storey buildings using cross-layer installed cable-bracing inerter systems: Part 1 theoretical treatment, Soil Dyn. Earthq. Eng. 164 (2023), 107639.
[5] L. Xie, M. Cao, N. Funaki, et al., Performance Study of an Eight-story Steel Building Equipped with Oil Dampers Damaged During the 2011 Great East Japan Earthquake Part 1: Structural Identification and Damage Reasoning, J. Asian Arch. Build. Eng. 14 (1) (2015) 181–188.
[6] M. Cao, L. Xie, H. Tang, et al., Performance Study of an Eight -story Steel Building Equipped with Oil Damper Damaged During the 2011 Great East Japan Earthquake Part 2: Novel Retroit Strategy, J. Asian Arch. Build. Eng. 15 (2) (2016) 303–310.
[7] K. Kasai, A. Mita, H. Kitamura, et al., Performance of Seismic Protection Technologies during the 2011 Tohoku-Oki Earthquake, Earthq. Spectra 29 (2013) S265–S293.
[8] Y. Tong, S. Xue, L. Xie, et al., Identification of a monitoring nonlinear oil damper using particle filtering approach, Mech. Syst. Sig. Process. 189 (2023), 110020.
[9] Y. Tong, S. Xue, L. Xie, et al., Damping evaluation of an eight-story steel building with nonlinear oil damper under strong earthquakes, J. Build. Eng. 67 (2023), 106004.
[10] A.P. Jeary, Damping in structures, J. Wind Eng. Ind. Aerodyn. 72 (1) (1997) 345–355.
[11] H. Su, X. Yang, L. Liu, et al., Identifying nonlinear characteristics of model-free MR dampers in structures with partial response data, Measurement 130 (2018) 362–371.
[12] Y. Lei, X. Yang, J. Huang, et al., Identification of model-free hysteretic forces of magnetorheological dampers embedded in buildings under unknown excitations using incomplete structural responses, Struct. Control Health Monit. 28 (5) (2021) e2715.
[13] Y. Zhao, B. Xu, B. Deng, et al., Hysteresis and dynamic loading nonparametric identification for multi-degree-of-freedom structures using an updated general extended Kalman filter and a Legendre polynomial model, Struct. Control Health Monit. 29 (11) (2022) e3088.
[14] X. Yang, H. Su, L. Liu, et al., Identification of the nonlinear characteristics of rubber bearings in model-free base-isolated buildings using partial measurements of seismic responses, J. Low Frequency Noise, Vibration Active Control 39 (3) (2020) 690–703.
[15] J. Hwang, A. Kareem, W. Kim, Estimation of modal loads using structural response, J. Sound Vib. 326 (3) (2009) 522–539.
[16] R. Ghanem, M. Shinozuka, Structural system identification I: Theory, J. Eng. Mech. (ASCE) 121 (2) (1995) 255–264.
[17] G. Kerschen, K. Worden, A. Vakakis, et al., Past, present and future of nonlinear system identification in structural dynamics, Mech. Syst. Sig. Process. 20 (3) (2006) 505–592.
[18] Y. Chan, A. Hu, J. Plant, A Kalman Filter Based Tracking Scheme with Input Estimation, IEEE Trans. Aerospace Electronic Syst. 15 (2) (1979) 237–244.
[19] R. Kalman, A New Approach to Linear Filtering and Prediction Problems, J. Basic Eng. 82 (1) (1960) 35–45.
[20] K. Xu, A. Mita, Maximum drift estimation based on only one accelerometer for damaged shear structures with unknown parameters, J. Build. Eng. 46 (2021), 103372.
[21] J. Hwang, S. Lee, P. Jihoon, Y. EunJong, Force identification from structural responses using Kalman filter, Materials 33 (2009) 257–266.
[22] J. Hwang, A. Kareem, H. Kim, Wind load identification using wind tunnel test data by inverse analysis, J. Wind Eng. Ind. Aerodyn. 99 (2011) 18–26.
[23] C. Ji, P. Tuan, H. Jang, A recursive least-squares algorithm for on-line 1-D inverse heat conduction estimation, Int. J. Heat Mass Transf. 40 (9) (1997) 2081–2096.
[24] P. Tuan, S. Lee, W. Hou, An efficient on-line thermal input estimation method using Kalman filter and recursive least square algorithm, Inverse Prob. Eng. 5 (4) (1997) 309–333.
[25] C. Ma, J. Chang, D. Lin, Input forces estimation of beam structures by an inverse method, J. Sound Vib. 259 (2) (2003) 387–407.
[26] C. Ma, P. Tuan, D. Lin, et al., A study of an inverse method for the estimation of impulsive loads, Int. J. Syst. Sci. 29 (6) (1998) 663–672.
[27] E. Lourens, E. Reynders, G.D. Roeck, et al., An augmented Kalman filter for force identification in structural dynamics, Mech. Syst. Sig. Process. 27 (2012) 446–460.
[28] F. Neats, J. Cuadrado, W. Desmet, Stable force identification in structural dynamics using Kalman filtering and dummy-measurements, Mech. Syst. Sig. Process. 50 (2015) 235–248.
[29] K. Maes, A. Smyth, G. Roeck, et al., Joint input-state estimation in structural dynamics, Mech. Syst. Sig. Process. 70–71 (2016) 445–466.
[30] M. Hassanabadi, A. Heidarpour, S. Azam, et al., A Bayesian smoothing for input-state estimation of structural systems, Comput. Aided Civ. Inf. Eng. 37 (3) (2022) 317–334.
[31] Y. Lei, C. Qi, S. Wang, A Smoothing EKF-UI-WDF Method for Simultaneous Identification of Structural Systems and Unknown Seismic Inputs without Direct Feedthrough, Struct. Control Health Monit. 6968598 (2023).
[32] J. Huang, X. Li, F. Zhang, et al., Identification of joint structural state and earthquake input based on a generalized Kalman filter with unknown input, Mech. Syst. Sig. Process. 151 (2021), 107362.
[33] J. He, X. Zhang, B. Xu, KF-Based Multiscale Response Reconstruction under Unknown Inputs with Data Fusion of Multitype Observations, J. Aerosp. Eng. 32 (4) (2019) 04019038.
[34] X. Zhang, H.e. Jia, Q.i. Meng, Study on KF-based responses reconstruction of nonlinear structure and external excitation identification, J. Build. Struct. 41 (11) (2020) 143–149.
[35] L. Liu, J. Zhu, Y. Su, et al., Improved Kalman filter with unknown inputs based on data fusion of partial acceleration and displacement measurements, Smart Struct. Syst. 17 (6) (2016) 903–915.
[36] L. Liu, Y. Su, J. Zhu, Y. Lei, Data Fusion Based EKF-UI for Real-Time Simultaneous Identification of Structural Systems and Unknown External Inputs, Measurement 88 (2016) 456–467.
[37] S. Gillijns, B. Moor, Unbiased minimum-variance input and state estimation for linear discrete-time systems, Automatica 43 (1) (2007) 111–116.
[38] S. Gillijns, B. Moor, Unbiased minimum-variance input and state estimation for linear discrete-time systems with direct feedthrough, Automatica 43 (5) (2007) 934–937.
[39] E. Lourens, C. Papadimitriou, S. Gillijns, et al., Joint input-response estimation for structural systems based on reduced-order models and vibration data from a limited number of sensors, Mech. Syst. Sig. Process. 29 (5) (2012) 310–327.
[40] K. Ikago, Y. Sugimura, K. Saito, et al., Modal Response Characteristics of a Multiple-Degree-Of-Freedom Structure Incorporated with Tuned Viscous Mass Dampers, J. Asian Arch. Build. Eng. 11 (2) (2012) 375–382.